

Eternal Inflation-deflation and Force Fields in the Multiverse

Ding-Yu Chung

chung@wayne.edu

This paper explains the origins of the inflation, the four normal force fields, and the extreme force fields. It proposes that the background of the multiverse is the homogeneous static universe, consisting of 11D (space-time dimensional) positive energy membrane and negative energy anti-membrane with the Planck energy as the vacuum energy. The only force in the multiverse background is the attractive pre-strong force, the predecessor of the strong force. Vacuum energy decreases with decreasing space-time number based on quantized varying speed of light. (The vacuum energy of 4D space-time is zero.) With such vacuum energy differences, the local dimensional oscillation between high and space-time dimensions results in eternal local inflation-deflation. (For our observable universe, such vacuum energy differences become the mass-energy differences for 4D elementary particles, including quarks, leptons, and gauge bosons.) Each region of the universe follows a particular path of the dimensional oscillation, leading to a particular set of force fields. For our universe, gravity appears in the first dimensional oscillation between the 11 D membrane and the 10 D string. The asymmetrical weak force appears in the asymmetrical second dimensional oscillation between the 10D particle and the 4D particle. Electromagnetism appears as the force in the transition between the first and the second dimensional oscillations. The cosmology explains the origins of the four forces. Under extreme conditions such as zero absolute temperature and extremely high pressure, the extreme force fields form for superconductor, the fractional quantum Hall effect, gravastar, supernova, neutron star, and gamma ray burst.

Introduction

This paper explains the origins of the inflation, the four normal force fields, and the extreme force fields. The base of the explanation consists of the four assumptions: the multiverse background, the object structure, the space structure, and the dimensional oscillation. Cosmology describes the eternal inflation-deflation by the dimensional oscillation in string theory. The particular path of the dimensional oscillation provides the origin of the four normal force fields (the strong force, gravity, electromagnetism, and the weak force). Beyond the four normal force fields and under extreme conditions such as zero absolute temperature and extremely high pressure, the extreme force fields form for superconductor, the fractional quantum Hall effect, gravastar, supernova, neutron star, and gamma ray burst. Part 1 includes assumptions and cosmology. Part 2 is for the normal force fields, and Part 3 deals with the extreme force fields.

Part I: Assumptions and Cosmology

1. *The Four Assumptions*

The four assumptions in the eternal inflation-deflation in the multiverse are the multiverse background, the object structure, the space structure, and the dimensional oscillation. The first assumption of this paper is that the multiverse background is the homogeneous static universe, consisting of 11D (space-time dimensional) positive energy membrane and negative energy anti-membrane, as proposed by Mongan [1]. The only force in the homogeneous static universe is the attractive pre-strong force, the predecessor of the strong force. It does not have gravity that causes instability and singularity [2], so the initial universe remains homogeneous, flat, and static. This initial universe provides the globally stable static background state for an inhomogeneous eternal universe in which local regions undergo inflation-deflation [2].

The second assumption is about the object structure [3], consisting of 11D membrane (3_{11}), 10D string (2_{10}), variable D particle ($1_{\leq 10}$), and empty object (0). The four stages in the evolution of our universe are the 11D membrane universe (the background), the dual 10D string universe, the dual 10D particle universe, and the dual 4D/variable D particle universe, involving of 11D membrane, 10D string, 10D particle, and 4D/variable ≤ 10 D particle, respectively.

Empty object corresponds to the anti-De Sitter bulk space in the Randall-Sundrum model [4]. The surrounding object can extend into empty object by the decomposition of space dimension as described by Bounias and Krasnoholovets [5]. For an example, 11D membrane (3_{11}) in the presence of empty space (0) decomposes into 10D string (2_{10}) surrounded by a virtue particle (1_1) attached to the space of 10D string.

$$3_{11} + 0_{11} \xrightarrow{\text{the decomposition}} 2_{10} 1_1 \quad (1)$$

The third assumption is about space structure [6][7], consisting of attachment space (denoted as 1) and detachment space (denoted as 0). Attachment space attaches to object permanently with zero speed or reversibly at the speed of light. Detachment space irreversibly detaches from the object at the speed of light. Attachment space relates to rest mass, while detachment space relates to kinetic energy. Different stages of our universe have different space structures.

The first three stages of the cosmic evolution do not have detachment space. The cosmic origin of detachment space is the cosmic radiation that initiates the big bang. Some objects in 4D-attachment space, denoted as 1_4 , convert into the cosmic radiation in 4D-detachment space, denoted as 0_4 . Cosmic radiation cannot permanently attach to a space.

$$\text{some objects in } 1_4 \xrightarrow{\text{the big bang}} \text{the cosmic radiation in } 0_4 \quad (2)$$

The combination of attachment space (1) and detachment space (0) results in miscible space, binary partition space, or binary lattice space for four-dimensional space-time.

$$(1)_n \text{ attachment space} + (0)_n \text{ detachment space} \xrightarrow{\text{combination}} (1)_n(0)_n \text{ binary lattice space, miscible space, or binary partition space} \quad (3)$$

Binary lattice space, $(1)_n(0)_n$, consists of repetitive units of alternative attachment space and detachment space. Thus, binary lattice space consists of multiple quantized units of attachment space separated from one another by detachment space. In miscible space, attachment space is miscible to detachment space, and there is no separation of attachment space and detachment space. Binary partition space, $(1)_n(0)_n$, consists of separated continuous phases of attachment space and detachment space.

Binary lattice space consists of multiple quantized units of attachment space separated from one another by detachment space. Binary lattice space slices an object into multiple quantum states separated from one another by detachment space. Binary lattice space is the space for wavefunction. In wavefunction,

$$|\Psi\rangle = \sum_{i=1}^n c_i |\phi_i\rangle \quad , \quad (4)$$

Each individual basis element, $|\phi_i\rangle$, attaches to attachment space, and separates from the adjacent basis element by detachment space. Detachment space detaches from object. Binary lattice space with n units of four-dimensional, $(0)_n(1)_n$, contains n units of basis elements.

Detachment space contains no object that carries information. Without information, detachment space is outside of the realm of causality. Without causality, distance (space) and time do not matter to detachment space, resulting in non-localizable and non-countable space-time. The requirement for the system (binary lattice space) containing non-localizable and non-countable detachment space is the absence of net information by any change in the space-time of detachment space. All changes have to be coordinated to result in zero net information. This coordinated non-localized binary lattice space corresponds to nilpotent space. All changes in energy, momentum, mass, time, space have to result in zero as defined by the generalized nilpotent Dirac equation [8].

$$(\mp \mathbf{k} \partial / \partial t \pm \mathbf{i} \nabla + \mathbf{j} m)(\pm i \mathbf{k} E \pm \mathbf{i} \mathbf{p} + \mathbf{j} m) \exp i(-Et + \mathbf{p} \cdot \mathbf{r}) = 0 \quad , \quad (5)$$

where E, \mathbf{p} , m, t and \mathbf{r} are respectively energy, momentum, mass, time, space and the symbols $\pm 1, \pm i, \pm \mathbf{i}, \pm \mathbf{j}, \pm \mathbf{k}, \pm \mathbf{i}, \pm \mathbf{j}, \pm \mathbf{k}$, are used to represent the respective units required by the scalar, pseudoscalar, quaternion and multivariate vector groups. The changes involve the sequential iterative path from nothing (nilpotent) through conjugation,

complexification, and dimensionalization. The non-local property of binary lattice space for wavefunction provides the violation of Bell inequalities [9] in quantum mechanics in terms of faster-than-light influence and indefinite property before measurement. The non-locality in Bell inequalities does not result in net new information.

In binary lattice space, for every attachment space, there is its corresponding adjacent detachment space. Thus, a basis element attached to attachment space can never be at rest with complete localization even at the absolute zero degree. The adjacent detachment space forces the basis element to de-localize.

In binary lattice space, for every detachment space, there is its corresponding adjacent attachment space. Thus, no part of the object can be irreversibly separated from binary lattice space, and no part of a different object can be incorporated in binary lattice space. Binary lattice space represents coherence as wavefunction. Binary lattice space is for coherent system. Any destruction of the coherence by the addition of a different object to the object causes the collapse of binary lattice space into miscible space. The collapse is a phase transition from binary lattice space to miscible space. Any destruction of the coherence by the addition of a different object to the object causes the collapse of binary lattice space into miscible space. The collapse is a phase transition from binary lattice space to miscible space.

$$\begin{array}{ccc} ((0)(1))_n & \xrightarrow{\text{collapse}} & \text{miscible space} \\ \text{binary lattice space} & & \end{array} \quad (6)$$

Another way to convert binary lattice space into miscible space is gravity. Penrose [10] pointed out that the gravity of a small object is not strong enough to pull different states into one location. On the other hand, the gravity of large object pulls different quantum states into one location to become binary partition space. Therefore, a small object without outside interference is always in binary lattice space, while a large object is never in binary lattice space.

In miscible space, attachment space is miscible to detachment space, and there is no separation of attachment space and detachment space. In miscible space, attachment space contributes zero speed, while detachment space contributes the speed of light. A massless particle, such as photon, is on detachment space continuously, and detaches from its own space continuously. For a moving massive particle consisting of a rest massive part and a massless part, the massive part with rest mass, m_0 , is in attachment space, and the massless part with kinetic energy, K , is in detachment space. The combination of the massive part in attachment space and massless part in detachment leads to the propagation speed in between zero and the speed of light.

To maintain the speed of light constant for a moving particle, the time (t) in moving particle has to be dilated, and the length (L) has to be contracted relative to the rest frame.

$$\begin{aligned}
t &= t_0 / \sqrt{1 - v^2 / c^2} = t_0 \gamma, \\
L &= L_0 / \gamma, \\
E &= K + m_0 c^2 = \gamma m_0 c^2
\end{aligned}
\tag{7}$$

where $\gamma = 1 / \sqrt{1 - v^2 / c^2}$ is the Lorentz factor for time dilation and length contraction, E is the total energy and K is the kinetic energy.

The information in miscible space is contributed by the combination of both attachment space and detachment space, so detachment space with information can no longer be non-localize. Any value in miscible space is definite. All observations in terms of measurements bring about the collapse of wavefunction, resulting in miscible space that leads to eigenvalue as definite quantized value. Such collapse corresponds to the appearance of eigenvalue, E , by a measurement operator, H , on a wavefunction, Ψ .

$$H \Psi = E \Psi \quad , \tag{8}$$

The fourth assumption [3] is about the dimensional oscillation between high dimensional space-time and low dimensional space-time. The vacuum energy of the multiverse background is the Planck energy. Vacuum energy decreases with decreasing dimension number. The vacuum energy of 4D space-time is zero. With such vacuum energy differences, the local dimensional oscillation between high and low space-time dimensions results in local eternal inflation-deflation. Eternal inflation-deflation is like harmonic oscillator, oscillating between the Planck vacuum energy and the lower vacuum energy.

$$V(\phi) = \frac{m^2}{2} \phi^2 \tag{9}$$

Eternal inflation-deflation starts with eternal inflation [11][12][13]. In eternal inflation, once inflation has started, it continues forever, producing an unlimited number of pocket universes. Such pocket universes correspond to the units of 11D membranes. Once inflation, all adjacent units of 11D membrane inflate into lower D entities. For the dimensional oscillation, deflation occurs at the end of inflation. Each local region in the universe follows a particular path of the dimensional oscillation. Each path is marked by particular set of force fields. The path for our universe is marked by the strong force, gravity-antigravity, charged electromagnetism, and asymmetrical weak force, corresponding to the four stages of the cosmic evolution.

Since the initial universe is flat and homogeneous, the dimensional oscillation changes from one flat-homogeneous state into another flat-homogeneous state. The universe requires overall flatness and homogeneity, and allows temporary local deviations from flatness and homogeneity. The universe does not need inflation to reach flatness and uniformity.

The vacuum energy differences among space-time dimensions are based on the varying speed of light. Varying speed of light has been proposed to explain the horizon problem of cosmology [14][15][16]. The proposal is that light traveled much faster in the distant past to allow distant regions of the expanding universe to interact since the beginning of the universe. Therefore, it was proposed as an alternative to cosmic inflation. The time dependent speed of light varies as some power of the expansion scale factor a in such way that

$$c(t) = c_0 a^n \quad (10)$$

where $c_0 > 0$ and n are constants. The increase of speed of light is continuous.

In this paper, varying dimension number (VDN) relates to quantized varying speed of light (QVSL), where the speed of light is invariant in a constant space-time dimension number, and the speed of light varies with varying space-time dimension number from 4 to 11.

$$c_D = c / \alpha^{D-4}, \quad (11)$$

where c is the observed speed of light in the 4D space-time, c_D is the quantized varying speed of light in space-time dimension number, D , from 4 to 11, and α is the fine structure constant for electromagnetism. Each dimensional space-time has a specific speed of light. The speed of light increases with the increasing space-time dimension number D .

In special relativity, $E = M_0 c^2$ modified by Eq. (11) is expressed as

$$E = M_0 \cdot (c^2 / \alpha^{2(D-4)}) \quad (12a)$$

$$= (M_0 / \alpha^{2(d-4)}) \cdot c^2. \quad (12b)$$

Eq. (12a) means that a particle in the D dimensional space-time can have the superluminal speed c / α^{D-4} , which is higher than the observed speed of light c , and has the rest mass M_0 . Eq. (12b) means that the same particle in the 4D space-time with the observed speed of light acquires $M_0 / \alpha^{2(d-4)}$ as the rest mass, where $d = D$. D in Eq. (12a) is the space-time dimension number defining the varying speed of light. In Eq. (12b), d from 4 to 11 is “mass dimension number” defining varying mass. For example, for $D = 11$, Eq. (12a) shows a superluminal particle in eleven-dimensional space-time, while Eq. (12b) shows that the speed of light of the same particle is the observed speed of light with the 4D space-time, and the mass dimension is eleven. In other words, 11D space-time can transform into 4D space-time with 11d mass dimension. QVSL in terms of varying space-time dimension number, D , brings about varying mass in terms of varying mass dimension number, d .

The QVSL transformation transforms both space-time dimension number and mass dimension number. In the QVSL transformation, the decrease in the speed of light leads to

the decrease in space-time dimension number and the increase of mass in terms of increasing mass dimension number from 4 to 11,

$$c_D = c_{D-n} / \alpha^{2n}, \quad (13a)$$

$$M_{0,D,d} = M_{0,D-n,d+n} \alpha^{2n}, \quad (13b)$$

$$D, d \xrightarrow{QVSL} (D \mp n), (d \pm n) \quad (13c)$$

where D is the space-time dimension number from 4 to 11 and d is the mass dimension number from 4 to 11. For example, the QVSL transformation steps a particle with 11D4d to a particle with 4D11d. In terms of rest mass, 11D space-time has 4d with the lowest rest mass, and 4D space-time has 11d with the highest rest mass.

Rest mass decreases with increasing dimension number. The decrease in rest mass means the increase in vacuum energy, so vacuum energy increases with increasing dimension number. The vacuum energy of 4D particle is zero, while 11D membrane has the Planck vacuum energy. Vacuum energy differences among 11D membrane, 10D string, and variable D particle produces inflation-deflation. For our observable universe, the vacuum energy differences become the mass-energy differences for 4D elementary particles, including quarks, leptons, and gauge bosons [17]. It provides the base for the periodic table of elementary particles to calculate accurately the masses of all 4D elementary particles in the observable universe.

Since the speed of light for $> 4D$ particle is greater than the speed of light for 4D particle, the observation of $> 4D$ particles by 4D particles violates casualty. Thus, $> 4D$ particles are hidden particles with respect to 4D particles. Particles with different space-time dimensions are transparent and oblivious to one another.

In the normal supersymmetry transformation, the repeated application of the fermion-boson transformation carries over a boson (or fermion) from one point to the same boson (or fermion) at another point at the same mass. In the “varying supersymmetry transformation”, the repeated application of the fermion-boson transformation steps a boson from one point to the boson at another point at different mass dimension number in the same space-time number. The repeated varying supersymmetry transformation carries over a boson B_d into a fermion F_d and a fermion F_d to a boson B_{d-1} , which can be expressed as follows

$$M_{d,F} = M_{d,B} \alpha_{d,B}, \quad (14a)$$

$$M_{d-1,B} = M_{d,F} \alpha_{d,F}, \quad (14b)$$

where $M_{d,B}$ and $M_{d,F}$ are the masses for a boson and a fermion, respectively, d is the mass dimension number, and $\alpha_{d,B}$ or $\alpha_{d,F}$ is the fine structure constant that is the ratio between the masses of a boson and its fermionic partner. Assuming $\alpha_{d,B}$ or $\alpha_{d,F}$, the relation between the bosons in the adjacent dimensions then can be expressed as

$$M_{d-1,B} = M_{d,B} \alpha_d^2. \quad (14c)$$

Eqs. (15) show that it is possible to describe mass dimensions > 4 in the following way

$$F_5 B_5 F_6 B_6 F_7 B_7 F_8 B_8 F_9 B_9 F_{10} B_{10} F_{11} B_{11}, \quad (15)$$

where the energy of B_{11} is the Planck energy. Each mass dimension between 4d and 11d consists of a boson and a fermion. Eqs. (15) show a stepwise transformation that converts a particle with d mass dimension to $d \pm 1$ mass dimension. The transformation from a higher dimensional particle to the adjacent lower dimensional particle is the fractionalization of the higher dimensional particle to the many lower dimensional particle in such way that the number of lower dimensional particles becomes $n_{d-1} = n_d / \alpha^2$. The transformation from lower dimensional particles to higher dimensional particle is a condensation. Both the fractionalization and the condensation are stepwise. For example, a particle with 4D (space-time) 10d (mass dimension) can transform stepwise into 4D9d particles. Since the supersymmetry transformation involves translation, this stepwise varying supersymmetry transformation leads to a translational fractionalization and translational condensation, resulting in expansion and contraction.

Another type of the varying supersymmetry transformation is not stepwise. It is the leaping varying supersymmetry transformation that transforms a particle with d mass dimension to any $d \pm n$ mass dimension. The transformation involves the slicing-fusion of particle. Bounias and Krasnoholovets [18] propose another explanation of the reduction of > 4 D space-time into 4D space-time by slicing > 4 D space-time into infinitely many 4D quantized units surrounding the 4D core particle. Such slicing of > 4 D space-time is like slicing 3-space D object into 2-space D object in the way stated by Michel Bounias as follows: “You cannot put a pot into a sheet without changing the shape of the 2-D sheet into a 3-D dimensional packet. Only a 2-D slice of the pot could be a part of sheet”.

In this paper, this slicing involves the slicing of mass dimensions. For example, the slicing of > 4 d particle is as follows.

$$\begin{array}{ccc} \left(1_{4+k} \right)_M & \xrightarrow{\text{slicing}} & \left(1_4 \right)_M + \sum_{k=1}^k \left(\left(0_4 \right) \left(1_4 \right) \right)_{N,k} \\ >4d \text{ attachment space} & & 4d \text{ core attachment space} \quad k \text{ types of } 4d \text{ units} \end{array} \quad (16)$$

The two products of the slicing are the 4d-core attachment space and k types of 4d quantized units. The 4d core attachment space surrounded by k types of infinitely many 4D4d quantized units corresponds to the core particle surrounded by k types of infinitely many small 4d particles.

Therefore, the transformation from d to $d - n$ involves the slicing of a particle with d mass dimension into two parts: the core particle with $d - n$ dimension and the n dimensions that are separable from the core particle. Such n dimensions are denoted as n

“dimensional orbitals”, which become force fields. The sum of the number of mass dimensions for a particle and the number of dimensional orbitals (DO’s) is equal to 11 for all particles with mass dimensions. Therefore,

$$F_d = F_{d-n} + (11-d+n) \text{ DO's} \quad (17)$$

where $11 - d + n$ is the number of dimensional orbitals (DO’s) for F_{d-n} . For example, the slicing of 4D11d particle produces 4D4d particle that has $d = 4$ core particle surrounded by 7 separable dimensional orbitals. Since the slicing process is not stepwise from higher mass dimension to lower mass dimension, it is possible to have simultaneous slicing. For example, 4D10d particles can simultaneously transform into 4D10d, 4D9d, 4D8d, 4D7d, 4D6d, 4D5d, and 4D4d core particles, which have 0, 1, 2, 3, 4, 5, and 6 separable dimensional orbitals, respectively.

Therefore, varying supersymmetry transformation can be stepwise or leaping. Stepwise supersymmetry transformation is translational fractionalization and condensation, resulting in stepwise expansion and contraction. Leaping supersymmetry transformation is not translational, and it is slicing and fusion, resulting possibly in simultaneous formation of different particles with separable dimensional orbitals.

In summary, the QVSL transformation carries over both space-time dimension number and mass dimension number. The varying supersymmetry transforms varying mass dimension number in the same space-time number as follows ($D =$ space-time dimension number and $d =$ mass dimension number).

$$\begin{aligned} D, d &\xrightarrow{QVSL} (D \mp n), (d \pm n) \\ D, d &\xrightarrow{\text{stepwise varying supersymmetry}} D, (d \pm 1) \\ D, d &\xrightarrow{\text{leaping varying supersymmetry}} D, (d \pm n) \end{aligned} \quad (18)$$

2. Cosmology

As in Einstein’s static universe, the time in the multiverse background has no beginning. Different parts of the background have potential to undergo local inhomogeneity to develop different universes with different object structures, space structures, and vacuum energies.

This paper proposes that the multiverse background is the 11D membrane universe consisting of the closely packed identical 11D positive energy membrane-negative energy antimembranes, denoted as $3_{11} 3_{-11}$. The only force among the membranes is the pre-strong force, s , as the predecessor of the strong force. It is from the quantized vibration of the membranes to generate the reversible process of the absorption-emission of the massless particles among the membranes. The pre-strong force mediates the reversible

absorption-emission in the flat space. The pre-strong force is the same for all membranes, so it is not defined by positive or negative sign. The expression for 11D membrane and the pre-strong force is $3_{11} s$.

In certain regions of the 11D membrane universe, the local inflation takes place by the transformation from 11D membrane into 10D string. The inflation is the result of the vacuum energy difference between 11D membrane and 10D string. With the emergence of empty space (0_{11}), 11D membrane transforms into 10D brane (string) warped with virtue particle as pregravity.

$$3_{11} s + 0_{11} \longleftrightarrow 2_{10} s 1_1 = 2_{10} s g^+ \quad (19)$$

The g is in the bulk space [4], which is the warped space (transverse radial space) around 2_{10} . As in the AdS/CFT duality [19][20][21], the pre-strong force has 10D dimension, one dimension lower than the 11D membrane, and is the conformal force defined on the conformal boundary of the bulk space. The pre-strong force mediates the reversible absorption-emission process in the flat space, while pregravity mediates the reversible condensation-decomposition process in the bulk space.

Through symmetry, antistrings form 10D antibranes with anti-pregravity as $2_{-10} g^-$, where g^- is anti-pregravity.

$$3_{-11} s + 0_{-11} \longleftrightarrow 2_{-10} s 1_{-1} = 2_{-10} s g^- \quad (20)$$

Pregravity can be attractive or repulsive to anti-pregravity. If it is attractive, the universe remains homogeneous. If it is repulsive, n units of $(2_{10})_n$ and n units of $(2_{-10})_n$ are separated from each other.

$$((s 2_{10}) g^+)_n (g^- (s 2_{-10}))_n \quad (21)$$

The universe with pregravity and anti-pregravity is the dual 10D string universe, which leads to the evolution of our observable universe. The dual 10D string universe consists of two parallel universes with opposite energies: 10D branes (strings) with positive energy and 10D antibranes (antistrings) with negative energy. The two universes are separated by the bulk space, consisting of pregravity and anti-pregravity. The continuous spread of the local inflation enlarges the dual 10D string universe by converting the surrounding 11D membrane universe continuously. Like the expansion of the observable universe, the enlargement of the dual 10D string universe has no one specific mass center in space-time. Such dual universe separated by bulk space appears in the ekpyrotic universe model [22][23].

When the local inflation stops, the pressure of the surrounding 11D membrane universe forces the dual 10D string universe to deflate, resulting in the coalescence of the two universes. The coalescence allows the two universes to mix. The first path of such mixing is the brane-antibrane annihilation, resulting in disappearance of the dual universe and the return to the multiverse background. The outcome is the completion of one oscillating cycle.

The second path is the emergence of the pre-charge force, the predecessor of electromagnetism with positive and negative charges. During the coalescence before the mixing, the positive pre-charge (e^+) is added to the positive energy brane, while the negative pre-charge (e^-) is added to the negative energy antibrane. The mixing becomes the mixing of positive charge and negative charge, resulting in the preservation of the dual universe with the positive energy and the negative energy, which do not form a mixture. Our universe follows the second path.

During the coalescence for the second path, the two universes coexist in the same space-time, which is predicted by the Santilli isodual theory [24]. Antiparticle for our positive energy universe is described by Santilli as follows, “this identity is at the foundation of the perception that antiparticles “appear” to exist in our space, while in reality they belong to a structurally different space coexisting within our own, thus setting the foundations of a “multidimensional universe” coexisting in the same space of our sensory perception” (Ref. 24, p. 94). Antiparticles in the positive energy universe actually come from the coexisting negative energy universe.

The mixing process follows the isodual hole theory that is the combination of the Santilli isodual theory and the Dirac hole theory. In the Dirac hole theory that is not symmetrical, the positive energy observable universe has an unobservable infinitive sea of negative energy. A hole in the unobservable infinitive sea of negative energy is the observable positive energy antiparticle.

In the dual 10D string universe, one universe has positive energy branes with pregravity, and one universe has negative energy antibranes with anti-pregravity. For the mixing of the two universes during the coalescence, a new force, the pre-charged force, emerges to provide the additional distinction between brane and antibrane. The pre-charged force is the predecessor of electromagnetism. Before the mixing, the positive energy brane has positive pre-charge (e^+), while the negative energy antibrane has negative pre-charge (e^-). During the mixing when two 10D string universes coexist, a half of positive energy branes in the positive energy universe move to the negative energy universe, and leave the Dirac holes in the positive energy universe. The negative energy antibranes that move to fill the holes become positive energy antibranes with negative pre-charge in the positive energy universe. In terms of the Dirac hole theory, the unobservable infinitive sea of negative energy is in the negative energy universe from the perspective of the positive energy universe before the mixing. The hole is due to the move of the negative energy antibrane to the positive energy universe from the perspective of the positive energy universe during the mixing, resulting in the positive energy antibrane with negative pre-charge in the positive energy universe.

In the same way, a half of negative energy antibranes in the negative energy universe moves to the positive energy universe, and leave the holes in the negative energy universe. The positive energy branes that move to fill the holes become negative energy branes with positive pre-charge in the negative energy universe. The result of the mixing is that both positive energy universe and the negative energy universe have branes-antibranes. The existence of the pre-charge provides the distinction between brane and antibrane in the brane-antibrane.

At that time, the space (detachment space) for radiation has not appeared in the universe [3], so the brane-antibrane annihilation does not result in radiation. The brane-antibrane annihilation results in the replacement of the brane-antibrane as the 10D string-antistring, $(2_{10} 2_{-10})$ by the brane-antibrane as the 10D particle-antiparticle $(1_{10} 1_{-10})$. The 10D particles-antiparticles have the multiple dimensional Kaluza-Klein structure with variable space dimension number without the requirement for a fixed space dimension number for string-antistring.

The dual 10D particle universe has particles, while the multiverse background (11D membrane universe) has membranes, so the multiverse background and the dual 10D particle universe are completely transparent and oblivious to each other. Without the pressure from the multiverse background, pregravity and anti-pregravity again separate the two universes, resulting in the dual 10D particle universe. The dual 10D particle universe is represented as below.

$$((s 1_{10} e^+ e^- 1_{-10} s) g^+)_n \quad (g^- (s 1_{10} e^+ e^- 1_{-10} s))_n, \quad (22)$$

where s and e are the pre-strong force and the pre-charged force in the flat space, g is pregravity in the bulk space, and $1_{10} 1_{-10}$ is the particle-antiparticle. The dual 10D particle universe consists of two parallel particle-antiparticle universes with opposite energies and the bulk space separating the two universes.

Without relation with the multiverse background, the dual 10D universe has its own vacuum energy that decreases from the non-zero to zero. With decreasing vacuum energy and the Kaluza-Klein structure without a fixed number of space dimensions, the space-time dimension and the mass dimension of particle-antiparticles decrease to lower dimensional space-time, leading to the inflation of the universe.

The transformation of 10D particles in the dual universe can be symmetrical or asymmetrical. In the symmetrical transformation, both universes have the same transformation in such way that the ten-dimensional space-time decreases dimension-by-dimension to the 4D space-time slowly, sequentially, and reversibly, or decreases to the 4D at once.

The transformation that leads to our observable universe is asymmetrical. It results from the emergence of the asymmetrical weak force, which has the spatially asymmetrical transformation from one particle to another particle. The vacuum energy of the positive energy universe decreases to zero at once, and the space-time dimension decreases to 4D at once. The vacuum energy of the negative energy universe decreases to zero slowly, and the space-time dimension decreases to 4D slowly and sequentially. The result is the dual 4D/variable D universe in the two different modes: the quick mode and the quick mode. As shown later, the 4D is the observable universe, while the variable universe is the hidden universe. The observable universe has detachment space, resulting in the emergence of light, so it is the light universe. The hidden universe does not have detachment space, so it is the dark universe.

In the dark universe, the 10D4d particles at high vacuum energy transform into 9D5d particles at lower vacuum energy and higher rest mass through the QVSL transformation. Through the varying supersymmetry transformation, 9D5d transforms into 9D4d. Such

varying supersymmetry transformation brings about the stepwise translational fractionalization, resulting in cosmic expansion. Further decrease in vacuum energy repeats the same process again until particles are the 4D particles at zero vacuum energy as follows

The Slow Mode: The Hidden Dark Universe and the Dark Energy Universe

$$10D4d \rightarrow 9D5d \rightarrow 9D4d \rightarrow 8D5d \rightarrow 8D4d \rightarrow 7D5d \rightarrow \bullet\bullet\bullet \rightarrow 5D4d \rightarrow 4D5d \rightarrow 4D4d$$

\mapsto *the hidden dark universe* \leftrightarrow *dark energy* \leftarrow

The dark universe consists of two periods: the hidden dark universe and the dark energy universe. The hidden dark universe composes of the > 4D particles. As mentioned before, since the speed of light for > 4D particle is greater than the speed of light for 4D particle, the observation of > 4D particles by 4D particles violates casualty. Thus, > 4D particles are hidden particles with respect to 4D particles. The universe with > 4D particles is the hidden dark universe. The 4D particles transformed from hidden > 4D particles in the dark universe are observable dark energy for the light universe, resulting in the accelerated expanding universe. The accelerated expanding universe consists of the positive energy 4D particles-antiparticles and dark energy that includes the negative energy 4D particles-antiparticles and the antigravity. Since the dark universe does not have detachment space, the presence of dark energy is not different from the presence of the high vacuum energy.

The quick mode is used in the light universe. Through zero vacuum energy, 10D4d particle transforms through the quick QVSL transformation quickly into 4D10d particles, leading to the inflation. At the end of the inflationary expansion, all 4D10d particles undergo simultaneous slicing to generate equally by mass into 4D10d, 4D9d, 4D8d, 4D7d, 4D6d, 4D5d, and 4D4d core particles. Baryonic matter is 4D4d, while dark matter consists of the other six types of particles (4D10d, 4D9d, 4D8d, 4D7d, 4D6d, and 4D5d). The mass ratio of dark matter to baryonic matter is 6 to 1 in agreement with the observation [25] showing the universe consists of 23% dark matter, 4% baryonic matter, and 73% dark energy. The incompatibility between dark matter and baryonic matter leads to the inhomogeneity, resulting in the formation of galaxies, clusters, and superclusters [26].

The mechanism for the simultaneous slicing of mass dimensions requires detachment space that slices mass dimensions. The dual universe consists of 10D particle-antiparticle. With the CP symmetry, 10D particle-antiparticle undergoes annihilation (implosion). Annihilation is the detachment of energy from the original position. The space is detachment space, and the detached energy is cosmic radiation. The particles with CP asymmetry remain as the particles (matter). The whole process becomes

The Quick Mode :The Light Universe

$$10D4d \xrightarrow{\text{quick QVSL transformation, inflation}} 4D10d \xrightarrow{\text{simultaneous slicing with detachment space}} \text{dark matter } (4D10d + 4D9d + 4D8d + 4D7d + 4D6d + 4D5d) + \text{baryonic matter } (4D4d) + \text{cosmic radiation}$$

\rightarrow *thermal cosmic expansion (the big bang)*

For baryonic matter, the slicing of mass dimensions is as follows.

$$\binom{1_{4+6}}{m} \xrightarrow{\text{slicing}} \binom{1_4}{m} + \sum_1^6 \binom{(0_4)(1_4)}{n,6} \quad (23)$$

4D > 4d attachment space 4D4d core attachment space 6 types 4D4d units

where 4 and 6 (for six gauge force fields) are d mass dimensions.

The two products of the slicing are the 4D4d-core attachment space and six types of 4D4d quantized units. The 4D4d core attachment space surrounded by six types of infinitely many 4D4d quantized units corresponds to the core particle surrounded by six types of infinitely many small 4D4d particles. The gauge force fields are made of such small 4D4d quantized virtual particles surrounding the core particle.

The six > 4d mass dimensions (dimensional orbitals) for the gauge force fields and the one mass dimension for gravity are as in Figure 1.

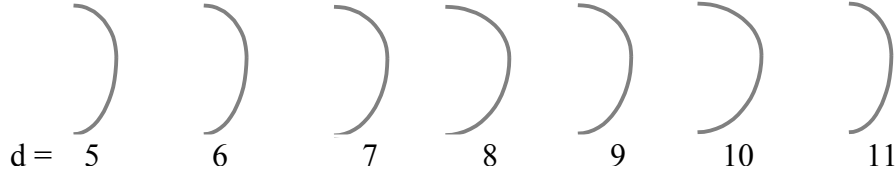


Figure 1. The force fields as > 4d mass dimensions (dimensional orbitals).

The dual 4D/variable D particle universe involves two distinctively different modes of the transformation (decay) from 10D to 4D, representing chirality of transformation. In the observable universe, such chirality is signified by the weak interaction (decay), involving the decay of particles with chirality. The dual 4D/variable D particle universe is as follows.

$$((s_{1_4} e^+ w^+ e^- w^- 1_{-4} s) g^+)_n (g^- (s_{1_{\le 10}} e^+ w^+ e^- w^- 1_{\ge -10} s))_n \quad (24)$$

where s, g, e, and w are the strong force, gravity, electromagnetism, and weak interaction, respectively for the observable universe, and where $1_4 1_{-4}$ and $1_{\le 10} 1_{\ge -10}$ are 4D particle-antiparticle for the observable universe and variable D particle-antiparticle for the hidden universe, respectively.

In summary, the whole process of the local inflation-deflation in the static universe is illustrated as follows.

$$\begin{array}{ccc}
\text{membrane universe} & \xrightarrow{\text{inflation-decomposition}} & \text{dual string universe} \xrightarrow{\text{deflation, coalescence, annihilation}} \\
3_{11} s s 3_{-11} & & ((s_{2_{10}}) g^+) (g^- (s_{2_{-10}}))_n \\
\\
\text{dual 10D particle universe} & \xrightarrow{\text{inflation-deflation}} & \text{dual 4D/variable D particle universe} \\
((s_{1_{10}} e^+ e^- 1_{-10} s) g^+) (g^- (s_{1_{10}} e^+ e^- 1_{-10} s))_n & & ((s_{1_4} e^+ w^+ e^- w^- 1_{-4} s) g^+) (g^- (s_{1_{\leq 10}} e^+ w^+ e^- w^- 1_{\geq -10} s))_n
\end{array}$$

where s , e , and w are in the flat space, and g is in the bulk space. Each stage generates one force, so the four stages produce the four different forces: the strong force, gravity, electromagnetism, and the weak interaction, sequentially. Gravity appears in the first dimensional oscillation between the 11 dimensional membrane and the 10 dimensional string. The asymmetrical weak force appears in the asymmetrical second dimensional oscillation between the ten dimensional particle and the four dimensional particle. Charged electromagnetism appears as the force in the transition between the first and the second dimensional oscillations. The cosmology explains the origins of the four forces.

The hidden universe with $D > 4$ and the observable universe with $D = 4$ are the “parallel universes” without any interaction between them. When the slow QVSL transformation of 5D hidden particles in the hidden universe into observable 4D particles, the observable 4 D particles become the dark energy for the observable universe. Physically, the observable universe gradually “swallows” the hidden universe including its energy density and negative pressure from anti-gravity, resulting in accelerated cosmic expansion. At a certain time, the hidden universe disappears, and becomes completely observable as dark energy. Afterward, 4D dark energy transforms back to $> 4D$ particles that are not observable. The removal of dark energy in the observable universe leads to the removal of energy density and negative pressure, resulting in the stop of accelerated expansion and the start of contraction of the observable universe.

The end of dark energy starts another “parallel universe period” without any interaction between them. Both hidden universe and observable universe contract synchronically. Eventually, gravity causes the observable universe to crush to lose all cosmic radiation, resulting in the return to 4D10d particles. The increase in vacuum energy (deflation) allows 4D10d particles to become positive energy 10D4d particles-antiparticle. Meanwhile, hidden $> 4D$ particles-antiparticles in the hidden universe transform into negative energy 10D4d particles-antiparticles. Both universes can undergo transformation by the reverse isodual hole theory to become dual 10D string universe, which in turn can return to the 11D membrane universe as the multiverse background as follows.

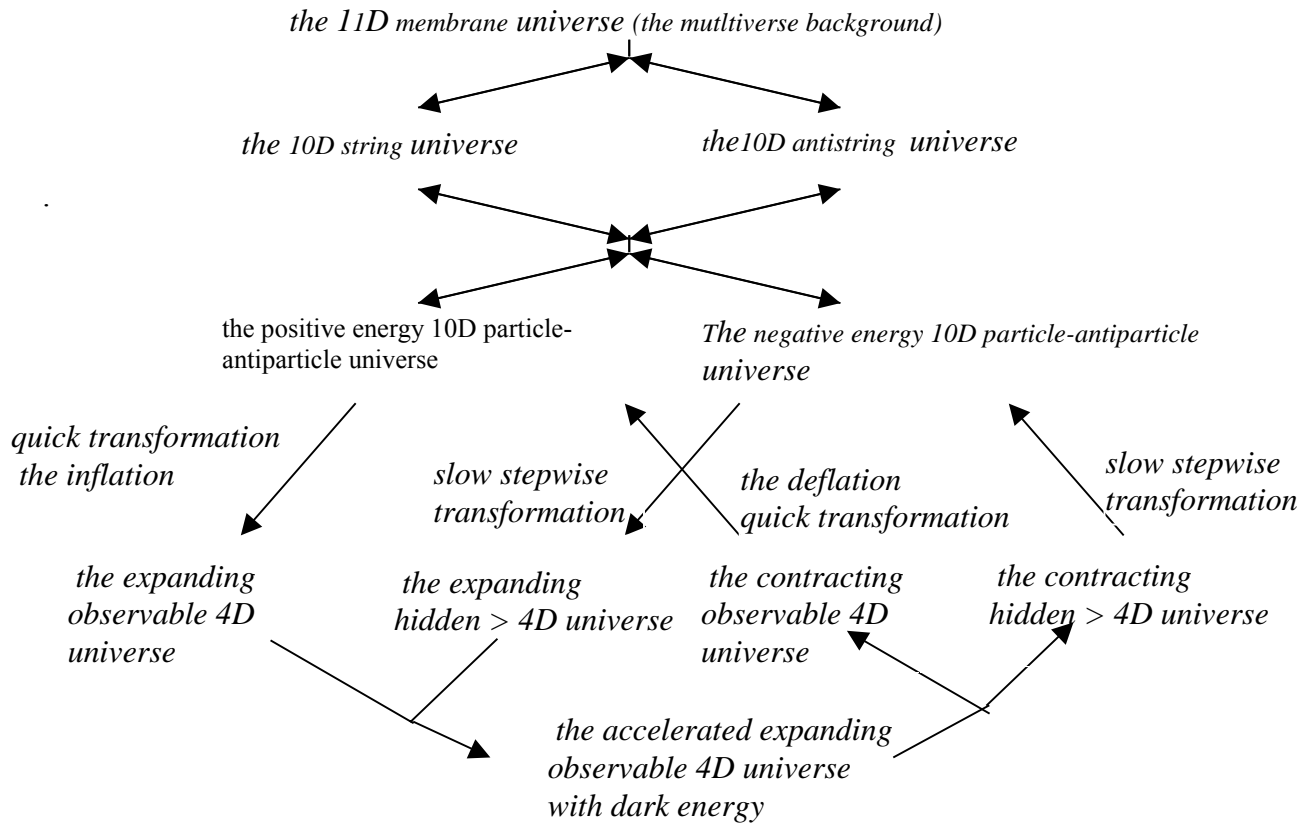


Figure 2. Cosmology

Part 2: The Normal Force Fields

3. *The Force Fields: the Masses of Gauge Bosons*

The second major part of the universal maturation process includes the force fields for our baryonic matter. It involves the dimensional orbital as in Fig. (1).

The structure of the 4d particle with dimensional orbitals resembles to the structure of atomic orbital. Consequently, the periodic table of elementary particles is constructed to account of all leptons, quarks, gauge bosons, and hadrons.

For the gauge bosons, the seven orbitals of principal dimensional orbital are arranged as $F_5 B_5 F_6 B_6 F_7 B_7 F_8 B_8 F_9 B_9 F_{10} B_{10} F_{11} B_{11}$, where B and F are boson and fermion in each orbital. The mass dimension in Eq. (14) becomes the orbitals in dimensional orbital with the same equations.

$$M_{d,F} = M_{d,B} \alpha_{d,B}, \quad (25a)$$

$$M_{d-1, B} = M_{d,F} \alpha_{d,F}, \quad (25b)$$

$$M_{d-1, B} = M_{d,B} \alpha_{d,B}^2, \quad (25c)$$

where D is the dimensional orbital number from 6 to 11. $E_{5,B}$ and $E_{11,B}$ are the energies for the 5d dimensional orbital and the 11d dimensional orbital, respectively. The lowest energy is the Coulombic field,

$$E_{5,B} = \alpha E_{6,F} = \alpha M_e \quad (26)$$

The bosons generated are the dimensional orbital bosons or B_D . Using only α_e , the mass of electron (M_e), the mass of Z^0 , and the number (seven) of dimensional orbitals, the masses of B_D as the gauge boson can be calculated as shown in Table 1.

Table 1. The Masses of the dimensional orbital bosons:

$\alpha = \alpha_e$, $d =$ dimensional orbital number

B_d	M_d	GeV (calculated)	Gauge boson	Interaction, symmetry	Predecessor
B_5	$M_e \alpha$	3.7×10^{-6}	A	Electromagnetic, U(1)	pre-charged
B_6	M_e / α	7×10^{-2}	$\pi_{1/2}$	Strong, $SU(3) \rightarrow U(1)$	pre-strong
B_7	$M_6 / \alpha_w^2 \cos \theta_w$	91.177 (given)	Z_L^0	weak (left), $SU(2)_L$	Fractionalization
B_8	M_7 / α^2	1.7×10^6	X_R	CP (right) nonconservation, $U(1)_R$	CP asymmetry
B_9	M_8 / α^2	3.2×10^{10}	X_L	CP (left) nonconservation, $U(1)_L$	CP asymmetry
B_{10}	M_9 / α^2	6.0×10^{14}	Z_R^0	weak (right), $SU(2)_R$	Fractionalization
B_{11}	M_{10} / α^2	1.1×10^{19}	G	gravity, D particle in D+1 bulk	Pregravity

In Table 1, $\alpha = \alpha_e$ (the fine structure constant for electromagnetic field), and $\alpha_w = \alpha / \sin^2 \theta_w$. α_w is not same as α of the rest, because as shown later, there is a mixing between B_5 and B_7 as the symmetry mixing between U(1) and SU(2) in the standard theory of the electroweak interaction, and $\sin \theta_w$ is not equal to 1. As shown later, B_5 , B_6 , B_7 , B_8 , B_9 , and B_{10} are A (massless photon), $\pi_{1/2}$ (half of pion), Z_L^0 , X_R , X_L , and Z_R^0 , respectively, responsible for the electromagnetic field, the strong interaction, the weak (left handed) interaction, the CP (right handed) nonconservation, the CP (left handed) nonconservation, and the P (right handed) nonconservation, respectively. The calculated value for α_w is 0.02973, and θ_w is 29.69° in good agreement with 28.7° for the observed value of θ_w [26]. The calculated energy for B_{11} is 1.1×10^{19} GeV in good agreement with the Planck mass, 1.2×10^{19} GeV.

There are dualities between dimensional orbitals and the cosmic evolution process. The pre-charged force, the pre-strong force, the fractionalization, the CP asymmetry, and the pregravity are the predecessors of electromagnetic force, the strong force, the weak interaction, the CP nonconservation, and gravity, respectively. These forces are manifested in

the dimensional orbitals with various space-time symmetries and gauge symmetries. The strengths of these forces are different than their predecessors, and are arranged according to the dimensional orbitals. Only the 4d particle (baryonic matter) has the B_5 , so without B_5 , dark matter consists of permanently neutral higher dimensional particles. It cannot emit light, cannot form atoms, and exists as neutral gas.

Quarks, leptons, and gauge bosons can be arranged in the periodical table of elementary particles, which can calculate the masses of elementary particles accurately. Details about quarks, leptons, and gauge bosons in the periodical table of elementary particles can be found in Reference 17.

Part 3: The Extreme Force Fields

4. *The quantum space phase transitions for force fields*

Under extreme conditions such as the absolute zero temperature or extremely high pressure, binary lattice space for a gauge force field undergoes a phase transition to become binary partition space for the extreme force fields.

At zero temperature or extremely high pressure, binary lattice space for a gauge force field undergoes a quantum space phase transition to become binary partition space. In binary partition space, detachment space and attachment space are in two separate continuous regions as follows.

$$\begin{array}{ccc} \left(1_4\right)_m + \sum_{k=1}^k \left(\left(0_4\right)\left(1_4\right)\right)_{n,k} & \longrightarrow & \left(1_4\right)_m + \sum_{k=1}^k \left(0_4\right)_{n,k} \left(1_4\right)_{n,k} \\ \text{particle} \quad \text{boson field} & & \text{hedge particle} \quad \text{hedgeboson field} \\ \text{in binary lattice space} & & \text{in binary partition space} \end{array} \quad (27)$$

The force field in binary lattice space is gauge boson force field, the force field in binary partition space is denoted as “hedge boson force field”. The detachment space in hedge boson field is the vacuum core, while hedge bosons attached to attachment space form the hedge boson shell. Gauge boson force field has no boundary, while the attachment space in the binary partition space acts as the boundary for hedge boson force field. Hedge boson field is like a bubble with core vacuum surrounded by membrane where hedge bosons locate.

The overlapping (connection) of two hedge bosons from two different sites results in “hedge bond”. The product is “hedge molecule”. An example of hedge molecule is Cooper pair, consisting of two electrons linked by hedge bond. Another example is superfluid, consisting of molecules linked by hedge bonds. Hedge bonds can be also formed among the sites in a lattice, resulting in hedge lattice. Hedge lattice is superconductor. Hedge boson force is incompatible to gauge boson force field. The

incompatibility of hedge boson force field and gauge boson force field manifests in the Meissner effect, where superconductor (hedge lattice) repels external magnetism. The energy (stiffness) of hedge boson force field can be determined by the penetration of boson force field into hedge boson force field as expressed by the London equation for the Meissner effect.

$$\nabla^2 H = -\lambda^{-2} H \quad , \quad (28)$$

where H is an external boson field and λ is the depth of the penetration of magnetism into hedge boson shell . This equation indicates that the external boson field decays exponentially as it penetrates into hedge boson force field.

5. *Superconductor and the Fractional Quantum Hall Effect*

Hedge boson exists only at the absolute zero temperature. However, quantum fluctuation at a temperature close to zero temperature allows the formation of a hedge boson. The temperature is the critical temperature (T_c). Such temperature constitutes the quantum critical point (QCP) [27]. Hedge boson at QCP is the base of superconductivity.

The standard theory for the conventional low temperature conductivity is the BCS theory. According to the theory, as one negatively charged electron passes by the positively charged ions in the lattice of the superconductor, the lattice distorts. This in turn causes phonons to be emitted which forms a channel of positive charges around the electron. The second electron is drawn into the channel. Two electrons link up to form the "Cooper pair" without the normal repulsion.

In the hedge boson model of the BCS theory, a hedge boson instead of a positive charged phonon is the link for the Cooper pair. According to the hedge boson model, as an electron passes the lattice of superconductor, lattice atom absorbs the energy of the passing electron to cause a lattice bond to stretch or to contract. When the lattice bond recoils to normal position, the lattice atom emits a phonon, which is absorbed by the electron. The electron then emits the phonon, which is absorbed by the next lattice atom to cause its bond to stretch. When the lattice bond recoils to normal position, the lattice atom emits a phonon, which is absorbed by the electron. The result is the continuous lattice vibration by the exchanges of phonons between the electrons in electric current and the lattice atoms in lattice.

At the temperature close to the absolute zero temperature, the lattice vibration continuously produces phonons, and through quantum fluctuation, a certain proportion of phonons converts to hedge bosons. Hedge bonds are formed among hedge bosons, resulting in hedge lattice. At the same time, the electrons involved in lattice vibration form hedge molecules as Cooper pairs linked by hedge bonds. Such hedge bond excludes electromagnetism, including the Coulomb repulsive force, between the two electrons. When Cooper pairs travel along the uninterrupted hedge bonds of a hedge lattice, Cooper pairs experience no resistance by electromagnetism, resulting in zero electric resistance. Hedge lattice repels external magnetism as in the Meissner effect.

The hedge bosons involved in the formation of the hedge lattice bonds and the hedge molecular bonds have the energy, so the hedge bond energy (E_l) for the hedge lattice is same as the hedge bond energy (E_c) for Cooper pair.

$$\begin{aligned} E_l &= E_c \\ &= 2\Delta_0 \end{aligned} \tag{29}$$

The hedge bond energy corresponds to two times the energy gap Δ_t at zero temperature in the BCS theory. The energy gap is the superconducting energy that an electron has. Δ_t approaches to zero continuously as temperature approaches to T_c . The elimination of superconductivity is to break the hedge bonds of the hedge lattice and Cooper pairs.

Hedge boson force is a confined short distant force, so the neighboring hedge bosons have to be close together. To have a continuous hedge lattice without gaps, it is necessary to have sufficient density of the vibrating lattice atoms. Thus, there is critical density, D_c , of vibrating lattice atoms. Below D_c , no hedge lattice can be formed. In a good conductor, an electron hardly interacts with lattice atoms to generate lattice vibration for hedge boson, so a good conductor whose density for vibrating lattice atoms below D_c does not become a superconductor. T_c is directly proportional to the density of vibrating lattice atoms and the frequency of the vibration (related to the isotope mass).

The “gap” in hedge lattice is the area without vibrating lattice atoms. The gap allows electric resistance. Superconductor has “perfect hedge lattice” without significant gap, while “imperfect hedge lattice” has significant gap to prevent the occurrence of superconductivity.

High temperature superconductor has a much higher T_c than low temperature superconductor described by the BCS theory. All high temperature superconductors involve the particular type of insulator with various kinds of dopants. A typical insulator is Mott insulator, such as copper oxides, CuO_2 . CuO_2 forms a two-dimensional layer, with the Cu atoms forming a square lattice and O atoms between each nearest-neighbor pair of Cu atoms. In the undoped CuO_2 , all of the planar coppers are in the Cu^{2+} state, with one unpaired electron per site. Two neighboring unpaired electrons with antiparallel spins have lower ground energy than two neighboring unpaired electrons with parallel spins. Two neighboring unpaired electrons with antiparallel spins constitute the antiparallel spin pair, which has lower ground state energy than the parallel spin pair. Consequently, CuO_2 layer consists of the antiparallel spin pairs, resulting in antiferromagnetism.

The insulating character of this state is thought to result, not from the antiferromagnetism directly, but from the strong on-site Coulomb repulsion, which is the energy cost of putting an extra electron on a Cu atom to make Cu^{1+} . This Coulomb energy for double occupancy suppresses conduction.

$\text{La}_x \text{Sr}_x \text{Cu}_2 \text{O}_4$ is an example of high temperature conductor. The key ingredient consists of CuO_2 layers. The doping of Sr provides chemical environment to shift the charge away from the CuO_2 layers, leaving “doping holes” in the CuO_2 layers. The shifting of electrons allows the occurrence of electric current. In the t-J model of high temperature

superconductor, an electron in electric current is fractionalized into two fractional electrons to carry spin quantum number in t and to carry charge in J [28].

$$H_{ij} = -t \sum_{ij\sigma} \tilde{c}_{i\sigma}^+ \tilde{c}_{j\sigma} + J \sum_{ij} \left[\vec{s}_i \cdot \vec{s}_j - \frac{n_i n_j}{4} \right] , \quad (30)$$

In the hedge boson model, t corresponds to the spin current (spinon) to generate spin fluctuation in the metal oxide layer, while J corresponds to the directional charge current (phonon as in the BCS theory) along the metal oxide layers. Hedge boson force field is a confined force field. As long as electrons are in the confined hedge boson force field, it is possible to have fractionalized electrons, similar to the fractionalized charges of quarks in the gluon force field.

The spin fluctuation generated by the spin current in the layer comes from doping holes in CuO_2 layer. When an antiparallel spin pair loses an electron by doping, a doping hole is in the spin pair. The adjacent electron outside of the pair fills in the hole. The filled-in electron has a parallel spin as the electron in the original pair. Parallel spin pair has higher ground state energy than antiparallel pair, so the filled-in electron absorbs a spinon to gain enough energy to undergo a spin change. The result is the formation of an antiparallel spin pair. The antiparallel spin pair has lower ground state energy than an antiparallel spin pair, so it emits a spinon. After the electron fills the hole, the hole passes to the next adjacent pair. The next adjacent pair then becomes the next adjacent newly formed parallel pair, which then absorbed the emitted spinon undergo spin change to form an antiparallel spin pair. The continuous passing of holes constitutes the layer spin current. The layer spin current throughout the CuO_2 layer generates the continuous spin fluctuation [29] with continuous emission and absorption of spinons.

At a low temperature, the spin fluctuation continuously produces spinons, and through quantum fluctuation, a certain proportion of spinons converts to hedge bosons. Hedge bonds are formed among hedge bosons. The hedge bonds are the parallel hedge bonds parallel to CuO_2 layer. The parallel hedge bond results from the spin current.

The hedge bonds connecting CuO_2 layers are the perpendicular bonds perpendicular to CuO_2 layers through d-wave by the lattice vibration, like the lattice vibration in the low temperature superconductor. The perpendicular bond results from the charge current. The perpendicular hedge bond energy (E_{\perp}) is greater than the parallel hedge bond energy (E_{\parallel}). Cooper pairs as the charge pairs travel along the perpendicular bonds. Thus, Cooper pair has the same bond as the perpendicular hedge bond. The hedge lattice consists of both parallel hedge bonds and perpendicular hedge bonds.

$$\begin{aligned} E_{II} &< E_{\perp} \\ E_c &= E_{\perp} \\ E_l &= E_{\parallel, \perp} \end{aligned} , \quad (31)$$

Perfect hedge lattice without gap of hedge bonds consists of both perfect parallel hedge lattice and perfect perpendicular hedge lattice without gaps for parallel hedge bonds and perpendicular bonds, respectively. The T_c of high temperature superconductor the transition temperature to the perfect hedge lattice, consisting of the perfect parallel hedge lattice and the perfect perpendicular lattice. Because many hedge bosons are generated from many spin fluctuations, T_c is high.

Having stronger hedge bond, the $T_{c\perp}$ for the perpendicular hedge lattice is higher than the $T_{c\parallel}$ for the parallel hedge lattice. Thus, T_c for the hedge lattice is essentially the $T_{c\parallel}$ for the parallel hedge lattice.

$$\begin{aligned} T_{c\parallel} &< T_{c\perp} \\ T_c &= T_{c\parallel} \end{aligned} \quad , \quad (32)$$

There are five different phases of metal oxide related to the presence or the absence of perfect parallel lattice, perfect perpendicular hedge lattice, and Cooper pairs as follows.

Table 2. The Phases of Metal Oxides

Phase/structure	perfect parallel hedge lattice	perfect perpendicular hedge lattice	Cooper pair
insulator	no	no	no
pseudogap	no	yes	yes
superconductor	yes	yes	yes
non-fermi liquid	no	no	yes
normal conductor	no	no	no

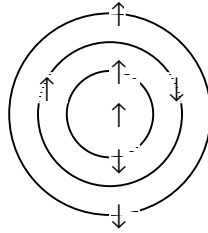
Without doping, metal oxide is an insulator. The pseudogap phase has a certain amount of doping. With a certain amount of doping, the perfect perpendicular hedge lattice can be established with the pseudogap transition temperature, T_p , equal to $T_{c\perp}$. However, the parallel lattice is imperfect with gaps, so it is not a superconductor. The pseudogap phase can also be achieved by the increase in temperature above T_c to create gap in the parallel hedge lattice, resulting in imperfect parallel hedge lattice. Different points in the pseudogap phase represent different degrees of the imperfect parallel hedge lattice. With the optimal doping, the pseudogap phase becomes the superconductor phase below T_c . Superconductor has perfect parallel hedge lattice and perfect perpendicular hedge lattice. With excessive doping, the superconductor phase becomes the conductor phase without significant spin fluctuation and lattice vibration. In the non-fermi liquid region, the hedge lattice is imperfect by the combination of the moderate increase in temperature above T_c and the moderate increase in doping. However, non-fermi liquid phase still has Cooper pairs that do not require the presence of perfect hedge lattice. In the

non-fermi liquid phase, due to the breaking of Cooper pairs with the increase in temperature, the transport properties are temperature dependent, unlike normal conductor.

In summary, for a low-temperature superconductor, hedge bosons are generated by the quantum fluctuation in lattice vibration by the absorption and the emission of phonons between passing electrons and lattice atoms. The connection of hedge bosons results in hedge lattice and Cooper pairs. For a high-temperature superconductor, hedge bosons are generated by the quantum fluctuation in spin fluctuation and lattice vibration by the absorption and the emission of spinons and phonons, respectively. The hedge lattice consists of the parallel hedge bonds and the perpendicular hedge bonds. Because many hedge bosons are generated from many spin fluctuations, T_c is high.

The hedge boson can also explain the fractional quantum Hall effect (FQHE) [30][31]. In the FQHE, electrons travel on a two-dimensional plane. In two-dimensional systems, the electrons in the direction of the Hall effect are completely separate, so the hedge bond cannot be formed between the electrons. However, an individual electron can have n hedge bosons from the quantum fluctuation of the magnetic flux at a very low temperature, resulting in hedge atom that consists of an electron and n hedge bosons with n hedge boson force fields.

Hedge boson force field consists of a core vacuum surrounded by only one hedge boson shell. An electron can be in $n \geq 1$ hedge boson force fields. If $n = 1$, an electron in a hedge boson force field delocalizes to the hedge boson shell, resulting in the probability distribution in both the center and the boson shell denoted as the hedge atomic orbital. (Unlike hedge boson force field, gauge boson force field can have infinite number of orbitals.) The probability distribution fractionalizes the electron into one fractional electron at the center and the $2p$ fractional electron in the hedge atomic orbital. Thus, the hedge atom ($n = p = 1$) has three fractional electrons, and each fractional electron has $-1/3$ charge. For $n > 1$, the multiple hedge force fields are like multiple separate bubbles with one fractional electron at the center. For $p=1$ and $n = 3$, the total number of fractional electrons is 7, and each fractional electron has $-1/7$ charge as follows.



The formulas for the number of fractional electrons and fractional charge are as follows.

$$\begin{aligned} \text{number of fractional electrons} &= 2pn + 1 \\ \text{electric charge } e &= -1 / (2pn + 1) \end{aligned} \quad , \quad (33)$$

where n = the hedge atomic orbital number and $2p$ = the number of hedge boson per orbital. The wavefunction of the hedge atom is as follows.

$$\Psi_n = \Phi \sum_n \left(\prod_{j < k} (z_j - z_k)^{2p} \right)_n, \quad (34)$$

where Φ is for the fractional electron at the center, $z_j = x_j - iy_j$, n = number of hedge atomic orbital, and $2p$ = number of fractional electrons per orbital. For the integer quantum Hall effect, $p = n = 0$. Eq. (34) is an electron in one or multiple hedge boson force fields. The probability distribution fractionalizes the electrons into the k fractional electron at the center (Φ) and the $2p j$ fractional electrons in the hedge atomic orbital. In Eq. (34), the j fractional electron in the hedge atomic orbital takes a loop around the k fractional electron at the center. One hedge boson force field can have only one hedge atomic orbital. When the electron is in multiple n hedge boson force fields, there are n separate hedge atomic orbitals with different sizes.

This wavefunction is same as same as the wavefunction of the composite fermion, which consists of an electron and $2p$ flux quanta [32]. In the composite fermion, Φ is the non-interacting electron and $2p$ is the number of flux quanta. The composite fermion is the bound state of an electron and $2p$ quantum vortices. In the same way, the hedge atom is the bound state of a fractional electron and $2pn$ fractional electrons in the hedge atomic orbitals. The hedge atomic orbital can be also described by the Laughlin-Jastrow factor by counting the centered fractional electron as a part of the hedge atomic orbital electrons, resulting in odd number of quasiparticles.

The hedge atoms provide the ground state for the Landau level. Within the ground state, the hedge atom with higher n and p has higher energy and lower probability. During the generation of the Landau levels, the fractional electrons come off the hedge atomic orbitals. The most favorable way is to remove one fractional electron per hedge atomic orbital to provide more room for the other fractional electron in the same hedge atomic orbital. For $n=1$, one $-1/3$ charged electron comes off. For $n=2$, two $-1/5$ charged electrons come off. The formula is $-n / (2n+1)$ electric charge as observed: $-1/3, -2/5, -3/7 \dots$ [33]. The second series is the leftover of the first series: $-2/3, -3/5, -4/7 \dots$

6. *Gravastar, Supernova, Neutron Star, and GRB*

Black hole has been a standard model for the collapse of a supermassive star. Two alternates for black hole are gravastar [34][35] and dark energy star [36]. Gravastar is a spherical void as Bose-Einstein condensate surrounded by an extremely durable form of matter. For dark energy star, the mass-energy of the nucleons under gravitational collapse can be converted to vacuum energy. The negative pressure associated with a large vacuum energy prevents the formation of singularity and results in an explosion. This paper proposes gravastar based on hedge boson field.

Before the gravitational collapse of large or supermassive star, the fusion process in the core of the star to create the outward pressure counters the inward gravitational pull of

the star's great mass. When the core contains heavy elements, mostly iron, the fusion stops. Instantly, the gravitational collapse starts. The great pressure of the gravity collapses atoms into neutrons. Further pressure collapses neutrons to quark matter and heavy quark matter.

Eventually, the high gravitational pressure transforms the gauge gluon force field into the hedge gluon force field, consisting of a vacuum core surrounded by a hedge gluon shell, like a bubble. The exclusion of gravity by the hedge gluon force field as in the Meissner effect prevents the gravitational collapse into singularity. In the Meissner effect for superconductor, a very strong magnetism can collapse the hedge boson force field, resulting in the disappearance of superconductivity. Superconductivity is based on quantum fluctuation between the gauge boson force field and the hedge boson force field, so it is possible to collapse the hedge boson force field. The formation of the hedge gluon force field is not by quantum fluctuation, so the hedge gluon force field cannot be collapsed. To keep the hedge gluon force field from collapsing, the vacuum core in the hedge gluon force field acquires a non-zero vacuum energy whose density (ρ) is equal to negative pressure (p). The space for the vacuum core becomes de Sitter space. The vacuum energy of the vacuum core comes from the gravitons in the exterior region surrounding the hedge gluon force field as in the Chapline's dark energy star. The external region surrounding the hedge gluon force field becomes the vacuum exterior region. Thus, the core of gravastar can be divided into three regions: the vacuum core, the hedge gluon shell, and the vacuum exterior region.

$$\begin{aligned}
 \text{vacuum core region: } \rho &= -p \\
 \text{hedge gluon shell region: } \rho &= +p \quad , \\
 \text{vacuum exterior region: } \rho &= p = 0
 \end{aligned}
 \tag{35}$$

Quarks without the strong force field are transformed into the decayed products as electron-positron and neutrino-antineutrino denoted as the "lepton composite".

$$\begin{aligned}
 \text{quarks} \xrightarrow{\text{quark decay}} e^- + e^+ + \bar{\nu} + \nu \\
 \text{the lepton composite}
 \end{aligned}
 \tag{36}$$

The result is that the core of the collapsed star consists of the lepton composite surrounded by the hedge gluon field. This lepton composite-hedge gluon force field core (LHC) constitutes the core for gravastar. The star consisting of the lepton composite-hedge gluon field core (LHC) and the matter shell is "gravastar". The matter shell consists of different layers of matters: heavy quark matter layer, quark matter layer, neutron layer, and heavy element layer one after the other.

LHC (*lepton composite – hedge gluon force field core*):

lepton composite region: $\rho = +p$

vacuum core region: $\rho = -p$

hedge gluon shell region: $\rho = +p$

vacuum exterior region: $\rho = p = 0$

Matter Shell: $\rho = +p$

heavy quark layer

quark layer

neutron layer

heavy element layer

(37)

The standard theory for supernova is that neutrinos released from nuclear fusion provide the energy needed to blow off the stellar mantle in a supernova, but details calculation shows that the neutrinos are too few and too weakly interacting for the required explosion [37].

In the hedge boson model, supernova is the lepton composite-powered exploding gravastar. The progenitor of supernova is a large star. The collapse of the star forms a gravastar with the LHC and the matter shell. Immediately after the formation of the gravastar, the matter shell derived from a large star does not have strong enough gravity to prevent the cracking of the matter shell by the outward pressure of the LHC. Through the cracks, the escaping lepton composite from the core becomes the “relativistic lepton composite” by adding kinetic energy converted from the non-zero vacuum energy of the hedge gluon force field. The relativistic lepton composite through the cracks explodes the heavy element layer of the matter shell, where gravity is weaker, and the crack is larger. The explosion is nearly symmetrical.

The inner part of the matter shell then collapses to form neutron star as the core remnant of supernova. The collapse of star initiates the rotation for neutron star with magnetic field. Pulsar is the rotational neutron star that contains a small remnant of the LHC after supernova.

The LHC remnant is large enough to crack the pulsar slightly. Through the small cracks, relativistic lepton composite leaks out continuously, and carries neutrons on the wall of the cracks to the surface of the magnetized rotational pulsar. The neutrons brought out by the relativistic lepton composite are highly energetic. These energetic neutrons quickly decay into protons and electrons, which rotate in the magnetic field. The energy that the particles carry by relativistic lepton composite accelerates the rotation of the pulsar. The rotating particles accelerate to the speeds approaching to the speed of light, resulting in synchrotron emission. The radiation is released as intense beams from the magnetic poles of the pulsar. The emitted radiation beam is rotated and sweeps regularly past the earth with precise period. The primary power source of the emitted radiation from pulsar is the

relativistic lepton composite, not the magnetic field. Therefore, a slow-rotating pulsar with a weak magnetic field can still maintain the emitted radiation.

The progenitor star of magnetar is much larger than the progenitor of an ordinary pulsar. During the supernova explosion, the high gravity of the large remnant neutron star attracts the debris to fall back on the remnant neutron star. The falling debris, mostly heavy elements, penetrates the remnant neutron star to form embedded heavy elements. The amount of embedded heavy elements increases with increasing mass with increasing gravity of the progenitor star. Since the progenitor of magnetar is large, it has a large amount of embedded heavy elements, weakening its structure, and causing large relativistic lepton composite-powered cracks in the matter shell. Large crack allows the release of high amount of relativistic lepton composite, so the emitted radiation includes high-energy X-ray from minor cracks and occasionally gamma ray burst from major cracks. Because of larger cracks, the disappearance of emitted radiation due to the disappearance of the relativistic lepton composite is quicker than ordinary pulsar.

The progenitor of GRB is a supermassive gravastar with millions sun masses. The matter shell in supermassive gravastar has strong enough gravity to prevent the cracks to disintegrate the matter shell by the outward pressure of the LHC. However, because of the outward pressure from the LHC, the supermassive gravastar is susceptible to crack by impact. The matter shell consists of the heavy quark matter layer, quark matter layer, neutron layer, and heavy element layer. Because of its large size, it has a large heavy element layer as the outer layer.

The GRB results from the volcano eruption initiated by the impact of a neutron star on a supermassive gravastar. The falling of a neutron star through the gravitational field of a gravastar generates high heat on the surface of the neutron star. Upon the impact, the heat of the neutron star liquefies the heavy elements on the surface of the gravastar into the “heavy element ocean”. The heat on the surface of the neutron star dissipates by the liquefaction. Then, the momentum of the neutron star breaks the heavy elements into large pieces, denoted as the “heavy element balls”. Finally, it reaches the neutron layer of the gravastar. The impact breaks the neutron star into large pieces, denoted as “the neutron balls”. The impact generates cracks into the LHC. Because of the extremely high gravity of the supermassive gravastar, all balls and liquid heavy elements are kept on the surface of the gravastar. Thus, the impact generates three layers (the heavy element ocean, the heavy element balls, and the neutron balls) and the cracks into the LHC.

Through the cracks generated by the impact, the escaping relativistic lepton composite through the cracks provides the kinetic energy to start the gravastar volcano eruption. First, the relativistic lepton composite carries the “heavy element material” (HEM) in the heavy element ocean in the form of the HEM jets to escape the gravity of the gravastar. There are many separated jets from many different cracks in a broad area, so it is a widespread volcano eruption. Soon, the heavy element ocean is almost dry.

At the same time, the flow of the relativistic lepton composite enlarges the cracks, resulting in increasing flow rate. The high flow rate of the relativistic lepton composite provides enough kinetic energy to carry the heavy element balls to escape the gravity of the gravastar. Each escaping ball has to have enough kinetic energy to escape from the gravity, so each jet can eject one heavy element ball in the interval of few minutes. The escaping

HEM forms the HEM band outside of the gravastar, while the heavy element balls form the heavy element ball band. At this time, the relativistic lepton composite is not strong enough to accelerate them to relativistic velocity. They remain non-relativistic. The HEM band eventually merges with the interstellar medium (ISM) to form a very thick layer of the HEM-ISM band.

The flow of the relativistic lepton composite further enlarges the cracks to increase the flow rate of the relativistic lepton composite. Eventually, the flow rate of the relativistic lepton composite is high enough to provide the kinetic energy for the neutron balls to escape the gravity of the gravastar. Each escaping ball has to have enough kinetic energy to escape from the gravity, so each jet can eject one neutron ball in the interval of few minutes. The neutron balls at this time are non-relativistic with the distance of few minutes between the adjacent neutron balls from the same jet. The escaping neutron balls form the neutron ball band.

Finally, the cracks are large enough to allow a huge amount of the relativistic lepton composite to eject from the volcano as the relativistic lepton composite jets. The relativistic lepton composite jets form the relativistic jet band. The initial ejecta composition is as in Fig. 3.

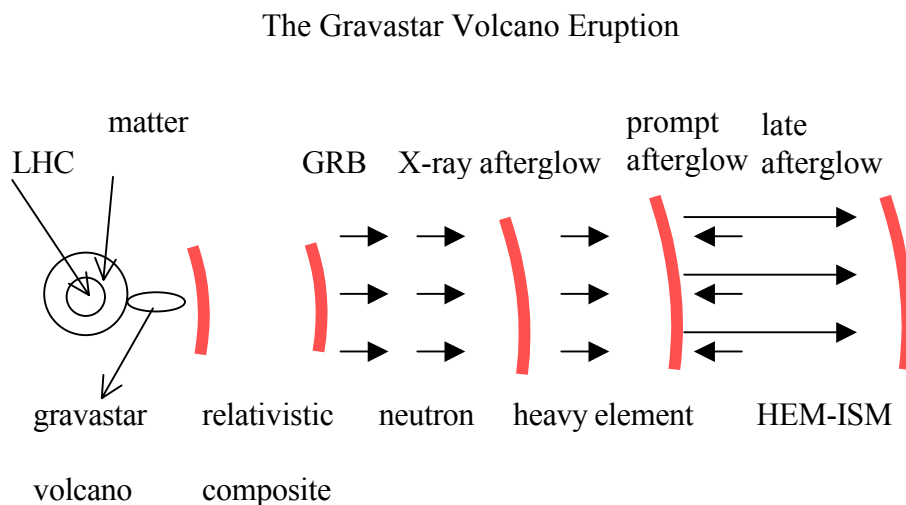


Fig. 3: The initial ejecta consists of the HEM-ISM band, the heavy element ball band, the neutron ball band, and the relativistic lepton composite jet band. The merges of various bands produce the GRB, the X-ray afterglow, the prompt afterglow, and the late afterglow in different regions.

The relativistic lepton composite jets sweep through all bands. The chance of being hit by the relativistic lepton composite jets decreases with the distance from the volcano. The majority of the relativistic jets accelerate the neutron balls to relativistic velocity, resulting in the relativistic neutron balls. The synchrotron emission by the acceleration from the relativistic neutron balls brings about the GRB. The acceleration of each neutron ball represents one burst. In the terms of the fireball model [38][39], the relativistic lepton

composite jet corresponds to the baryon-free fireball providing the kinetic energy for the internal and external shocks.

The volcano eruption depletes the relativistic lepton composite in a gravastar. Eventually, the pressure from the depleted source of the relativistic lepton composite becomes too low to prevent the collapse of the cracks by the gravitational pressure in the interior part of gravastar. The emission of the relativistic lepton composite through the volcano starts to decline sharply. Finally, all interior cracks collapse, and the major volcano eruption stops. The major volcano eruption lasts from 2 seconds to few minutes. (The high gravitational pressure replenishes the lepton composite afterward.) However, the volcano continues to eject the residual relativistic lepton composite as the weak residual relativistic lepton composite jets for few hours to few days. The weak residual relativistic lepton composite jets are not strong enough to cause further GRB.

After the stop of the major volcano eruption, the relativistic neutron balls start to collide with the non-relativistic neutron balls ahead. The closest non-relativistic neutron ball is few minutes ahead as the interval for the ejection of neutron ball during the volcano eruption. The collision between the relativistic neutron ball and the non-relativistic neutron ball leads to the deceleration, resulting in the synchrotron emission for the X-ray afterglow.

During the major volcano eruption, when the volcano ejects the neutron balls, the relativistic lepton composite enlarges not only the cracks vertically to the LHC but also the cracks in the heavy element layer on the shore of the heavy element ocean horizontally. After while, the flow rate of the relativistic lepton composite is high enough to eject large pieces of heavy element material on the shore of the ocean as the heavy element balls. These ejected heavy element balls are off-centered from the center where the neutron balls are ejected. Thus, the volcano ejects the off-centered heavy element balls along with the centered neutron balls in the late stage of the neutron ball ejection. The off-centered heavy element balls accelerated by the relativistic lepton composite jets become the off-centered relativistic heavy element balls. The density and the mass of the neutron ball are high, so the velocity of the relativistic neutron ball is lower than the relativistic heavy element ball. The off-centered heavy element balls occur later than the centered neutron balls, so the number of the heavy element balls is lower than the number of the neutron balls, resulting in the lower number density of the off-centered heavy element balls than the centered neutron balls.

As results, the centered relativistic neutron balls have lower velocity and higher number density than the off-centered relativistic heavy element balls. After the stop of the major volcano eruption, the low number density and off-centered heavy element balls collide first with the non-relativistic balls in the off-centered area of the neutron ball band. Because of the low number density, the slope for the number of collision is steep. Then, the centered relativistic neutron balls collide with the non-relativistic balls in the centered area of the neutron ball band. Because of the high number density, the slope for the number of collision is shallow.

The remaining relativistic balls without collisions in the neutron ball band collide with the non-relativistic balls in the heavy element ball band. These off-centered faster relativistic heavy element balls collide before the centered slower relativistic neutron balls.

Therefore, there are four different types of collisions to produce X-ray afterglow in the four different time periods as shown in Fig. 4.

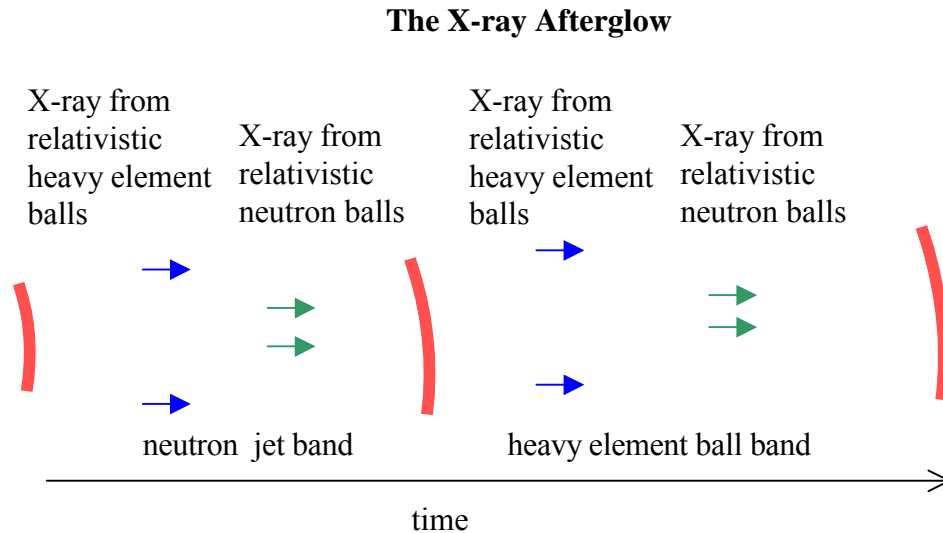


Fig. 4: There are the four types of the collisions to generate the X-ray afterglow in the order of occurrences. The first one is the collisions between the off-centered relativistic heavy element balls and the non-relativistic balls. The second one is the collisions between the centered relativistic neutron balls and the non-relativistic balls. The third one is the off-centered relativistic heavy element balls and the non-relativistic balls. The fourth one is the centered relativistic neutron balls and the non-relativistic balls.

The time periods overlap, but in a certain time period (especially the first and the second periods), one type of collisions dominates. They are the four distinct regions for the four different types of collisions as in the observed X-ray lightcurve [40]. A brief renewing of the volcano eruption during the early part of the X-ray afterglow accelerates the balls to bring about a sharp increase of X-ray emission (X-ray flare) from the synchrotron emission.

The leftover relativistic lepton composite from the collisions with the balls is the free relativistic lepton composite, which has considerable lower intensity than the relativistic lepton composite in the origin relativistic lepton composite jets. It reaches the HEM-ISM band slightly ahead the GRB that requires time for acceleration. The thick HEM-ISM reflects considerable amount of relativistic lepton composite as the “reverse shock” traveling backward. Soon after, the stop of the major volcano eruption causes the steep decline in the intensity of the relativistic lepton composite, so for a short time, the strong reverse shock traveling backward dominates the weak “forward shock” from the relativistic lepton composite under steep decline in intensity, resulting in a net reverse shock. The net reverse shock is followed by the weak forward shock from the weak residual relativistic lepton composite jets for few hours to few days as shown in Fig. 5.

The Net Reverse Shock and the Net Forward Shock

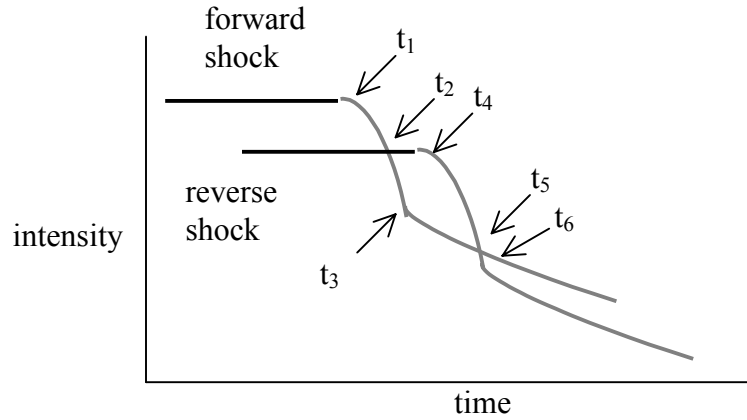


Fig. 5: The top curve is the intensity-time curve for the forward shock, and the bottom curve is the identical curve with lower intensity and later time for the reverse shock. t_1 = the start of the end of the eruption, t_2 = the start for the net reverse shock, t_3 = the start of the residual relativistic lepton composite jet, t_4 = the peak for the net reverse shock, t_5 = the end for net reverse shock and the start for the net forward shock, and t_6 = the peak for the net forward shock

In Fig. 5, the top curve is the intensity-time curve for the forward shock, and the bottom curve is the identical curve with lower intensity and later time for the reverse shock. At t_1 , the eruption starts steep decline. At t_2 , the net reverse shock starts to appear. At t_3 , the residual relativistic lepton composite jet starts. At t_4 , the net reverse shock reaches the peak. At t_5 , the net reverse shock disappears, and the net forward shock starts to appear. At t_6 , the net forward shock reaches the peak followed by the decline in intensity from the continuously declining residual relativistic lepton composite jets. Therefore, both the net reverse shock and the net forward shock have peaks in the intensity-time curves.

The main emissions for the net reverse shock and the net forward shock are the HEM-ISM emissions by the shocks. The emissions are the prompt afterglow by the net reverse shock and the late afterglow by the net forward shock. They are mostly UV, optical, IR, and radio wave. The net reverse shock has lower frequency than the net forward shock due the reduction of frequency during the reflection, so the prompt afterglow has lower frequency emissions than the late afterglow.

If the net reverse shock is in region of the HEM-ISM band far away from the heavy element ball band, the net reverse shock sweeps the region in the HEM-ISM band to generate emissions from the HEM-ISM. Then, the net forward shock sweeps the same region to generate emissions from the HEM-ISM. In this case, the only factor involved in the lightcurves is their intensity-time curves with two distinct peaks in agreement with the observation [40]. It is categorized as the “re-brightening” type with two distinctive peaks.

If the net reverse shock is in the region of the HEM-ISM band near the heavy element ball band, the late part of the net reverse shock is in the heavy element ball band.

In the heavy element ball band, there is very few HEM-ISM. Thus, no detectable HEM-ISM emission occurs in the late part of the net reverse shock. The peak of the net forward shock is likely buried in the heavy element ball band as shown in the observation [40]. It is categorized as the “flattening:” type without the peak for the net forward shock. If the net reverse shock appears in the heavy element ball band, no HEM emission by the net reverse shock occurs, resulting in the absence of the prompt afterglow [40].

The length of the ball bands and the length of the effective free relativistic lepton composite jets determine the location of the reverse shock. They relate to Poynting flux and the kinetic energy in the relativistic balls, respectively in the fireball model [40]. The strong reverse shock emission requires the location of the reverse shock in the high-density area of the HEM-ISM band and far away from the heavy element ball band.

When the neutron balls enter the HEM-ISM band, they decay, and leave trails of hydrogen. The trail of hydrogen becomes the factory for amino acid. Hydrogen reacts with carbon, nitrogen, and oxygen to form methane, ammonia, and water, respectively. The combination of photon, hydrogen, methane, ammonia, and water forms amino acids as in the 1950 experiment by Stanley Miller. The highly polarized light during the GRB provides the chirality for the formation of handed amino acids. The heavy element balls trap and carry the amino acids. Many billion years after, one of them provides the source of life on the earth.

A similar volcano eruption in a small scale can take place on a giant magnetar as soft gamma ray repeaters (SGR) [41][42]. It is the short GRB that lasts less than 2 seconds with much less intrinsic brightness and total emission than the long GRB. A giant magnetar has the LHC remnant and a significant amount of embedded heavy elements. Before a major volcano eruption, the cracks develop under a large embedded heavy element segment. The relativistic lepton composite fills the cracks. Eventually, the relativistic lepton composite breaks the embedded heavy element segment into pieces, and ejects them. The volcano ejects first the small pieces of heavy element as the HEM jets, and then ejects the large pieces as the heavy element balls. A part of the neutron body is also ejected as the neutron balls. Finally, the volcano ejects the accumulated relativistic lepton composite as the relativistic lepton composite jets. After that, the whole process of the GRB and the afterglow take place.

In summary, the impact of a neutron star on a supermassive gravastar causes cracks, initiating the relativistic lepton composite-powered volcano eruption. The volcano ejects the heavy element materials, the heavy element balls, the neutron balls, and the relativistic lepton composite jets sequentially. The relativistic lepton composite jets accelerate the neutron balls into the relativistic neutron balls, resulting in the GRB. After the GRB, the collisions between the relativistic neutron balls and the non-relativistic balls result in the X-ray afterglow. After the stop of the volcano eruption, the volcano continues to eject the weak residual relativistic lepton composite jets for few days. The combination of the original strong relativistic lepton composite jets during the eruption and the weak residual relativistic lepton composite jets after the eruption brings about the net reverse shock and the net forward shock for the prompt afterglow and the late afterglow, respectively. The short GRB is the small-scale volcano eruption on a giant magnetar.

The long GRB is a rare event. The collisions with the large objects other than neutron stars do not lead to the GRB. They cause the minor volcano eruptions on the gravastar, resulting in the supernova-like emissions, which are not observable from large cosmological distances. The supermassive gravastar is likely at the center of galaxy. In the early universe, the collision between the gravastar and a neutron star or other large objects occurred often, resulting in high frequency of the gravastar volcano eruption. Such high frequency of the gravastar volcano eruption is a major power source of quasars. Quasars are believed to be the most remote objects in the universe. The earliest quasars detected so far are about 700 millions years after the big bang. The closest quasars detected so far are about 800 millions light years away. Despite their small size they produce tremendous amounts of light and microwave radiation. The power source of quasars is not much bigger than the solar system, but they pour out 100 to 1,000 times as much light as a typical galaxy containing a hundred billion stars. A major power source of quasars is from the repetitive gravastar volcano eruptions.

7. Summary

This paper explains the origins of the inflation, the four normal force fields, and the extreme force fields. It proposes that the background of the multiverse is the homogeneous static universe, consisting of 11D (space-time dimensional) positive energy membrane and negative energy anti-membrane with the Planck energy as the vacuum energy. The only force in the multiverse background is the attractive pre-strong force, the predecessor of the strong force. Vacuum energy decreases with decreasing space-time number based on quantized varying speed of light. (The vacuum energy of 4D space-time is zero.) With such vacuum energy differences, the local dimensional oscillation between high and space-time dimensions results in eternal local inflation-deflation. (For our observable universe, such vacuum energy differences become the mass-energy differences for 4D elementary particles, including quarks, leptons, and gauge bosons.) Each region of the universe follows a particular path of the dimensional oscillation, leading to a particular set of force fields. For our universe, gravity appears in the first dimensional oscillation between the 11 D membrane and the 10 D string. The asymmetrical weak force appears in the asymmetrical second dimensional oscillation between the 10D particle and the 4D particle. Electromagnetism appears as the force in the transition between the first and the second dimensional oscillations. The cosmology explains the origins of the four forces.

Under extreme conditions, such as the zero temperature and extremely high pressure, the extreme force fields as hedge boson force fields form. The formation of the hedge molecule (the Cooper pair) and the hedge lattice provides the mechanism for the phase transition to superconductivity, while the formation of hedge atom with electron-hedge boson provides the mechanism for the phase transition to the fractional quantum Hall effect. The formation of the hedge gluon force field provides the mechanism for the phase transition to gravastar from a collapsing star. Gravastar consists of the lepton composite-hedge gluon force field core and the matter shell. Unlike black holes, gravastars continue to appear as neutron stars and the sources for gamma ray bursts. Neutron star is a

remnant gravastar after the explosion (supernova) of a large gravastar. A supermassive gravastar with cracks undergoes the “volcano eruption” as gamma ray bursts.

References

* chung@wayne.edu P.O. Box 180661, Utica, Michigan 48318, USA

- [1] T. R. Mongan, *General Relativity and Gravitation* 33 (2001) 1415 [gr-qc/0103021]; *General Relativity and Gravitation* 37 (2005) 967 [gr-qc/0501014]
- [2] J. D. Barrow, G. F. R. Ellis, R. Maartens, and C. G. Tsagas, *Class Quantum Grav.* 20 (2003), L155 [gr-qc/0302094]
- [3] D. Chung and V. Krasnoholovets, [physics/0512026]
- [4] L. Randall and R. Sundrum, *Phys.Rev.Lett.* 83 (1999) 4690 [hep-th/9906064]
- [5] M. Bounias and V. Krasnoholovets, *The Int. J. Systems and Cybernetics* 32, (2003) 1005-1020 [physics/0301049]
- [6] V. Krasnoholovets, and D. Y. Chung, *International Journal of Anticipatory Computing Systems* (2006), ed. by D. Dubois, 191-197
- [7] D. Chung, D. and V. Krasnoholovets, V., *Progress in Physics* 4 (2006) 74
- [8] B. M. Diaz and P. Rowlands, *American Institute of Physics Proceedings of the International Conference of Computing Anticipatory Systems* (2003), ed. Daniel Dubois
- [9] J. S. Bell, *Physics* 1 (1964), 195
- [10] R. Penrose, *Mathematical Physics* (2000) eds: by A. Fokas, A. Grigoryan, T. Kibble & B. Zegarliniski (Imperial College, London), pp. 266-282.
- [11] A. H. Guth, *Phys. Rev. D* 23 (1981) 347
- [12] A. Vilenkin, *Phys. Rev. D* 27 (1983) 2848
- [13] A. Linde, *A. Phys Lett B* 175 (1986) 395
- [14] J. Moffat, *Int. J. Mod. Phys. D* 2 (1993) 351 [gr-qc/9211020]
- [15] A. Albrecht and J. Magueijo, *Phys.Rev. D* 59 (1999) 043516 [hep-ph/9811018]
- [16] J. D. Barrow, *Phys. Lett. B* 564 (2003) 1, [gr-qc/0211074]
- [17] D. Chung, *Speculations in Science and Technology* 20 (1997) 259 [hep-th/0111147]
- [18] M. Bounias and V. Krasnoholovets, *The Int. J. Systems and Cybernetics* 32, no. 7/8, (2003) 945-975 [physics/0211096]
- [19] J. Maldacena, *Adv. Theor. Math. Phys. V. 2* (1998) 231 [hep-th/9711200]
- [20] S. S. Gubser, I. R. Klebanov, and A. M. Polyakov, *Phys. Lett.B* v. 428 (1998) 105 [hep-th/9802109]
- [21] E. Witten, *Adv. Theor. Math. Phys. V. 2* (1998) 253 [hep-th/9802150]
- [22] P. J. Steinhardt and N. Turok, *Phys.Rev. D* 65 (2002) 126003 [hep-th/0111098]
- [23] J. Khoury, Invited talk at the 6th RESCEU Symposium, 2003, [astro-ph/0401579]
- [24] R. M. Santilli, *Isodual theory of antimatter with applications to antigravity, grand unification, and cosmology* (Kluwer Academic Publishers, Boston/Dordrecht/London) 2006.

- [25] C. L. Bennett et al, *Astrophys.J.Suppl.* 148 (2003) 1, [astro-ph/0302207]
- [26] D. Chung, hep-th/0112036
- [27] P. Coleman and A. Schofield, *Nature* 433 (2005) 226
- [28] P. W. Anderson, P. A. Lee, M. Randeria, T. M. Rice, N. Trivedi, and F. C. Zhang
Phys.: Condens. Matter 16 (2004) R755-R769, cond-mat/0311467
- [29] A. Ramsak and P. Prelovsek, *P. Proc. of SPIE* (2005) 59320G-2, cond-
mat/0506726
- [30] D. C. Tsui, H. L. Störmer, and A. C. Gossard, *Phys. Rev. Lett.* 48 (1982) 1559-
1562
- [31] R. B. Laughlin, *Phys. Rev. Lett.* 50 (1983) pp 1395-1398
- [32] J. K. Jain, *Phys. Rev. Lett.* 63 (1989) pp. 199-202
- [33] H. Stormer, *Physica B* 177 (1992) pp. 401-408.
- [34] P. O. Mazur and E. Mottola, "Gravitational condensate stars: An alternative to black
holes", preprint LA-UR-01-5067 (2001) [gr-qc/0109035]
- [35] P. O. Mazur and E. Mottola, *Proc. Nat. Acad. Sci.* 111 (2004) pp. 9545-9550 [gr-
qc/0407075]
- [36] G. Chapline, *Proceedings of the Texas Conference on Relativistic Astrophysics*,
Stanford, CA, December, 2004 [astro-ph/0503200]
- [37] H. A. Bethe, *Rev. Mod. Phys.* 62 (1990), pp. 801-866
- [38] B. Zhang and P. Mészáros, *Int. J. Mod. Phys. A* 19 (2004) pp. 2385-2472
(arXiv:astro-ph/0311321)
- [39] T. Piran, , *Rev. Mod. Phys.* 76 (2005), pp. 1143-1210 [astro-ph/0405503]
- [40] B. Zhang, *Proc. of "Astrophysics Sources of High Energy Particles and Radiation"*
(eds. T. Bulik, G. Madejski and B. Rudak), Torun, Poland, 20-24 June, 2005 [astro-
ph/0509571]
- [41] E. Nakar, T. Piran, and R. Sari, *Astrophys. J.* 635 (2005) 516 [astro-ph/0502052]
- [42] A. Dar, *Chin.J.Astron.Astrophys.* 6 (2006) 323 [astro-ph/0509257]